PARAMETRIC IMAGING OF SOLID TUMORS USING AVERAGE SCATTER SIZE AND ACOUSTIC CONCENTRATION

M. L. Oelze[+], J. F. Zachary[#], and W. D. O'Brien, Jr.[+]

+ Bioacoustics Research Laboratory, Department of Electrical and Computer Engineering, University of Illinois, Urbana, IL USA

Department of Veterinary Pathobiology, University of Illinois, Urbana, IL USA

oelze@uiuc.edu

Abstract

Two kinds of solid tumors were acquired and scanned *in vivo* ultrasonically. The fibroadenoma was acquired from rats that had spontaneously developed mammary tumors. The carcinoma was acquired by culturing a 4T1-MMT carcinoma cell line in culture media and injecting the cancer cells into BALB/c mice. The scatterer properties of average scatterer diameter and acoustic concentration were estimated using a Gaussian form factor from the backscattered ultrasound. The parametric images showed a clear distinction between the two kinds of tumors. A statistically significant difference was observed between the estimated scatterer properties in the fibroadenoma and the carcinoma. The average scatterer diameter and acoustic concentration for the fibroadenomas were estimated at $105+/-14$ µm and $-15.6+/-5$ dB (mm^{-3}), respectively. The average scatterer diameter and acoustic concentration for the carcinomas was estimated to be $28+/-4.6$ µm and $10.6+/-6.9$ dB (mm^{-3}), respectively.

Introduction

The frequency-dependent information contained in the backscattered RF signal is not utilized by conventional B-mode imaging, and has been hypothesized to contain information about tissue microstructure [1,2]. The models have allowed estimates of average scatterer properties (size, shape and scatter strength) of tissue microstructure from backscattered RF signals for purposes of detecting and classifying tissues [2,3]. Specifically, parametric imaging based on ultrasound backscatter has been used to extract the average scatterer sizes and acoustic concentrations (product of the number concentration of scatterers times the relative impedance difference between the scatterers and surrounding tissues) for the classification of ocular tumors [4], prostate [5], liver [1], and renal tissue [6].

The present study compares two kinds of mammary tumors using scatterer property estimates and parametric imaging, viz., a spontaneous rat mammary tumor (fibroadenoma), and a mouse carcinoma mammary tumor implanted from cultured cells. Comparison between the microstructure of the two tumors is made using ultrasound parametric imaging and light microscopy.

Methods

Rat Fibroadenomas

Eight Sprague-Dawley rats (Harlan) that had developed spontaneous mammary tumors were evaluated. Each rat was euthanized with CO_2, and the tumor and surrounding area were shaved with electric clippers and depilated. The rat was placed on a holder in a tank of degassed water at 37°C for scanning with a single-element transducer. The transducer had a center frequency of 10 MHz, an aperture diameter of 12 mm, a focus at 100 mm, and a –6 dB pulse/echo bandwidth of 8 MHz measured from the reference spectrum. Estimates of scatterer properties were made within the depth of focus of the transducer.

The pulse/echo data acquisition procedure has been previously described [7]. Sampling rate of the received signals was 200 MHz. The attenuation assumed for the rats was 0.9 dB/cm/MHz.

After scanning, the tumors were excised, fixed in 10% neutral-buffered formalin, processed and stained with hematoxylin and eosin stain for routine histologic evaluation by light microscopy. The tumors were diagnosed as fibroadenomas following histopathologic evaluation. The tumor consisted of well-differentiated epithelial cells arranged in acini surrounded by bands of fibrous connective tissue.

Mouse Carcinomas

A mouse mammary tumor cell line (4T1 [CRL-2539], ATCC, Manassas, VA) was chosen because of its homogeneous cytologic characteristics. These cells were relatively uniform in morphology, oval to polygonal in shape with large prominent nuclei. Extracellular matrix was minimal to nonapparent. We used these cells as an *in vivo* model for homogeneous tissue scatterers.

4T1 cells were stored at -70°C, thawed at 37°C in a water bath, grown in RPMI 1640 medium with 10% fetal bovine serum (FSB) and antibiotic/antifungal supplements, and incubated at 37°C at 100% humidity and 5% CO_2. Cells were grown in 75 cm^2 tissue culture flasks. When cells were 80% confluent, they were rinsed with RPMI 1640 medium lacking FBS or supplements and then covered with 2.0 mL of Trypsin-EDTA to detach the cells from the flask. The cells were gently and repetitively drawn through a 10-mL pipette to individualize the cells. The number of cells present in an 80% confluent flask was determined to be approximately 1×10^7 cells/mL.

Detached cells were washed two times with 10 mL of RPMI 1640 medium lacking FBS or supplements and resuspended in RPMI 1640 medium lacking FBS or supplements to concentration of 1×10^5 cells/mL. The abdominal mammary fat pad of anesthetized [ketamine hydrochloride (87.0 mg/kg) and xylazine (13.0 mg/kg)] 8 to 16 week old female BALB/c mice (Harlan) was injected with 0.1 mL of suspended 4T1 cells (1×10^4 cells total). The number of cells injected initiated tumor growth in 100% of mice within 8-10 days post-injection. Tumors with a diameter of 1.0 cm or greater were used for parametric imaging.

For each of the 20 mice, the tumor and surrounding area were shaved with electric clippers and depilated. The mouse was placed on a holder in a tank of degassed water at 37˚C for scanning with a single-element transducer.

One of the transducers had a center frequency of 10 MHz, an aperture diameter of 12 mm, a focus at 50 mm, and a –6 dB pulse/echo bandwidth of 8 MHz measured from the reference spectrum. The other transducer had a center frequency of 20 MHz, an aperture diameter of 6 mm, a focus at 22 mm, and a –6 dB pulse/echo bandwidth of 15 MHz measured from the reference spectrum. Estimates of scatterer properties were made within the depth of focus of the transducers.

The pulse/echo data acquisition procedure has been previously described [7]. Sampling rate of the received signals was 200 MHz. The attenuation assumed for the mice was 0.4 dB/cm/MHz.

After scanning, the tumors were excised, fixed in 10% neutral-buffered formalin, processed and stained with hematoxylin and eosin stain for routine histologic evaluation by light microscopy. The tumors consisted of the carcinoma cells with relatively uniform morphology and minimal extracellular matrix. The cells were oval to polygonal in shape with prominent nuclei and cell bodies 50% to 200% larger than the nuclei.

Estimation Routines

The scatterer property estimates were made by comparing the backscattered power spectrum of the RF signal gated from each region-of-interest (ROI) to a theoretical backscattered power spectrum [2,8,9]. The Gaussian form factor was used to model the scattering properties of many soft tissues [1,2,8,10]. The measured backscattered power spectrum was compensated for attenuation losses [11]. The average scatterer diameter and the acoustic concentration were estimated.

Results

Figures 1 and 2 show several parametric images enhanced by the average scatterer size and average acoustic concentration, respectively, of the two kinds of tumors. A clear distinction is seen between the mouse carcinomas and the rat fibroadenomas in the parametric images enhanced by the estimated average scatterer size and average acoustic concentration. The average scatterer diameter and acoustic concentration for the fibroadenomas were estimated at $105 +/- 14$ μm and $-15.6 +/- 5$ dB (mm^{-3}), respectively. The average scatterer diameter and acoustic concentration for the carcinomas (20 MHz) was estimated to be $28 +/- 4.6$ μm and $10.6 +/- 6.9$ dB (mm^{-3}), respectively. For the 10 MHz carcinoma data, the average scatterer diameter and acoustic concentration was estimated to be $39.8 +/- 6.4$ μm and $21.3 +/- 5.9$ dB (mm^{-3}), respectively.

A statistically significant difference (ANOVA, $p < 0.05$) between scatterer diameter estimates from the rat fibroadenomas and mouse carcinomas was observed. Likewise, a statistically significant difference between scatterer acoustic concentration estimates from the rat fibroadenomas and mouse carcinomas was observed.

Figure 3 is a feature analysis plot where the estimated acoustic scatterer concentration *vs*. the estimated scatterer sizes for the 8 rats and the 20 mice. Two sets of data for the carcinomas were measured using two different transducers with center frequencies of 10 MHz (10 carcinomas) and 20 MHz (10 carcinomas). The 20-MHz estimates should represent better estimates because the *ka* range is more optimal for making estimates than from the 10-MHz transducer (*ka* range from 0.4 to 0.8 for 20 MHz as opposed to 0.2 to 0.4 for 10 MHz). The 20-MHz data gave smaller and more consistent scatterer size estimates, showing the importance of optimizing the *ka* range.

Discussion

Eight rats with spontaneous mammary tumors and 20 mice with tumors developed from a transplantable carcinoma cell line were examined ultrasonically. Estimates of properties of the tissue microstructure were made from the frequency dependence of the ultrasound backscatter. Parametric images were constructed that superimposed color-coded pixels related to the estimates of the scatterer properties of the average scatterer diameter and acoustic concentration. The study showed that parametric imaging based on estimated scatterer properties was able to distinguish between two kinds of solid tumors in rats and mice.

A clear distinction was seen between the fibroadenoma and the carcinoma tumors based on the scatterer property estimates. A statistical difference was seen between the fibroadenoma and carcinoma tumor for both scatterer size estimates and acoustic concentration estimates. The average scatterer size

estimates were largest in the fibroadenomas and smallest in the carcinomas. The comparison of average scatterer acoustic concentration between the two kinds of tumors showed that the acoustic concentration was largest with the carcinomas. The parametric images also reflect the distinction between the two kinds of tumors. The differences suggest that measurement of the estimated scatterer properties may be useful in discerning between different tissue types and that parametric imaging using the scatterer property estimates may be an important diagnostic tool.

Acknowledgements

References

[1] F. L. Lizzi, M. Ostromogilsky, E. J. Feleppa, M. C. Rorke, and M. M. Yaremko, "Relationship of ultrasonic spectral parameters to features of tissue microstructure," *IEEE Trans. Ultrason. Ferroelect. Freq. Cont.*, **33**, 319-329 1986.

[2] M. F. Insana, R. F. Wagner, D. G. Brown, and T. J. Hall, "Describing small-scale structure in random media using pulse-echo ultrasound," *J. Acoust. Soc. Am.*, **87**, 179-192 1990.

[3] M. F. Insana and T. J. Hall, "Parametric ultrasound imaging from backscatter coefficient measurements: image formation and interpretation," *Ultrason Imaging*, **12**, 245-267 1990.

[4] E. J. Feleppa, F. L. Lizzi, D. J. Coleman, and M. M. Yaremko, "Diagnostic spectrum analysis in ophthalmology: a physical perspective," *Ultrasound Med. Biol.*, **12**, 623-631 1986.

[5] E. J. Feleppa, T. Liu, A. Kalisz, M. C. Shao, N. Fleshner, and V. Reuter, "Ultrasonic spectral-parameter imaging of the prostate," *Int. J. Imaging Syst. Technol.*, **8**, 11-25 1997.

[6] M. F. Insana, J.G. Wood, and T.J. Hall, "Identifying acoustic scattering sources in normal renal parenchyma *in vivo* by varying arterial and ureteral pressures," *Ultrasound Med. Biol.*, **17**, 613-626 1991.

[7] M. L. Oelze, J. F. Zachary, and W. D. O'Brien, Jr., "Parametric imaging of rat mammary tumors *in vivo* for the purposes of tissue characterization," *J. Ultrasound Med.*, **21**, 1201-1210 2002.

[8] F. L. Lizzi, M. Astor, T. Liu, C. Deng, D. J. Coleman, and R. H. Silverman, "Ultrasonic spectrum analysis for tissue assays and therapy evaluation," *Int. J. Imaging Syst. Technol.*, **8**, 3-10 1997.

[9] J. A. Zagzebski, Z. F. Lu and L. X. Xao, "Quantitative ultrasound imaging: *In vivo* results in normal liver," *Ultrason. Imaging*, **15**, 335-351 1993.

[10] M. F. Insana, "Modeling acoustic backscatter from kidney microstructure using an anisotropic correlation function," *J. Acoust. Soc. Am.*, **97**, 649-655 1995.

[11] M. L. Oelze and W.D. O'Brien, Jr. "Frequency-dependent Attenuation-compensation Functions for Ultrasonic Signals Backscattered from Random Media," *J. Acoust. Soc. Amer.*, **111**, 2308-2319 2002.
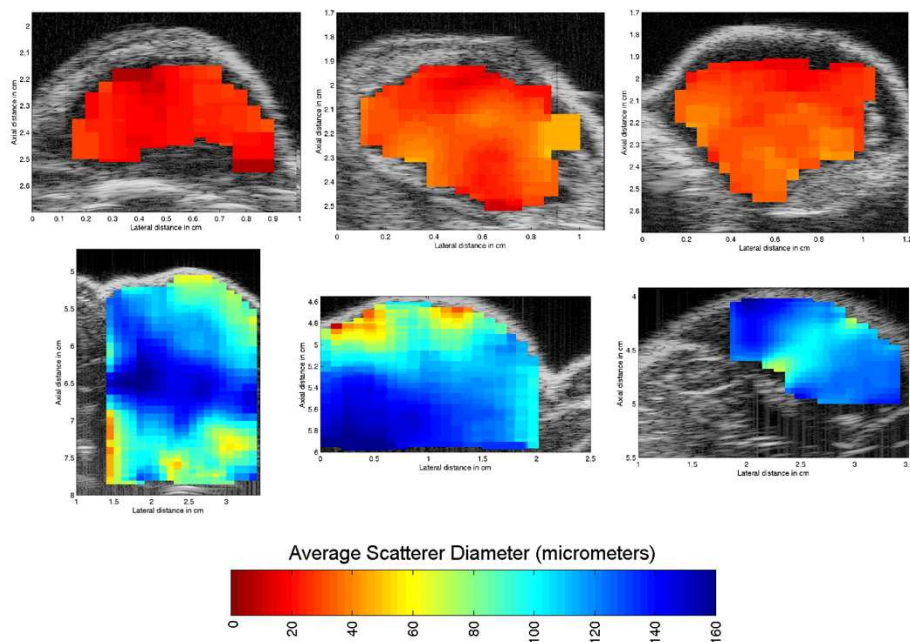
Figure 1: Parametric images of mouse carcinomas (top panel) made at 20 MHz and rat fibroadenomas (middle panel) using the estimated average scatterer size. The colorbar (bottom panel) shows the relation between the color-coded pixels and the average scatterer sizes.
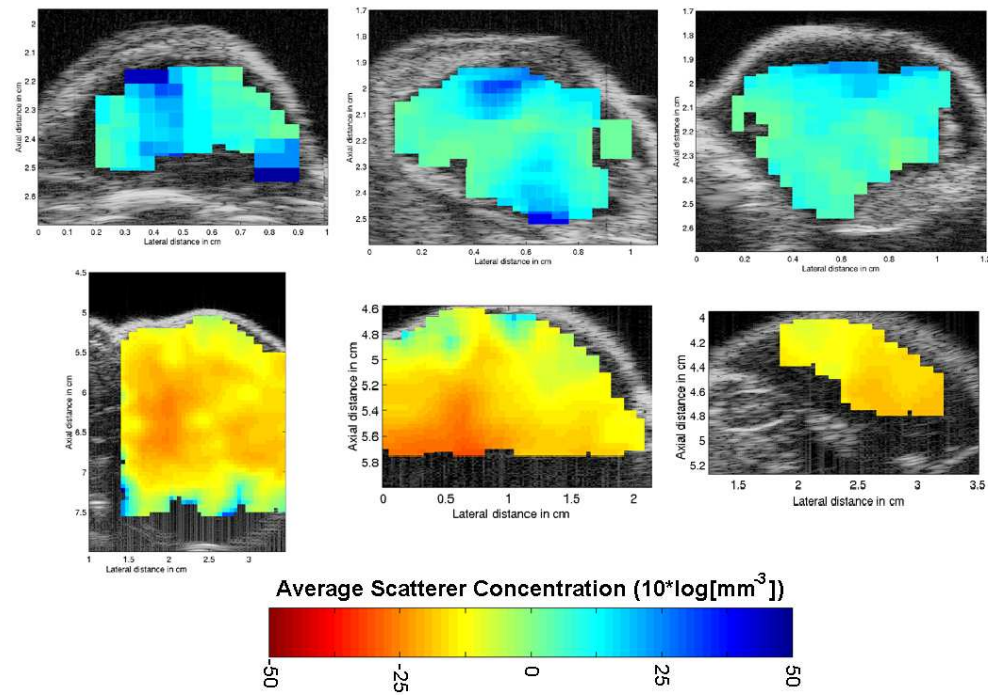
Figure 2: Parametric images of mouse carcinomas (top panel) made at 20 MHz and rat fibroadenomas (middle panel) using the estimated average acoustic concentration. The colorbar (bottom panel) shows the relation between the color-coded pixels and the average acoustic concentration.
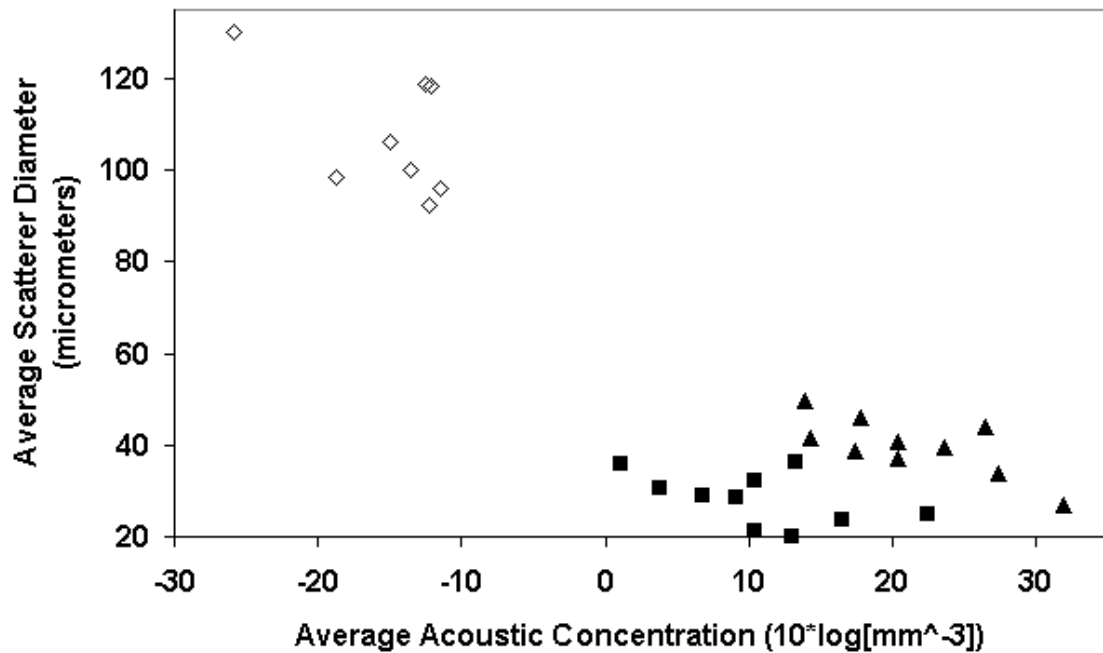

Figure 3: Feature analysis plot of the average scatterer acoustic concentration versus the average scatterer diameter for estimates made. Open diamond denotes inside the fibroadenomas. Filled-in square denotes inside the carcinomas (10 MHz). Filled-in triangle denotes inside the carcinomas (20 MHz).